

Organizational Results Research Report

September 2008
OR09.009

Preservation of Missouri Transportation Infrastructures: Validation of FRP Composite Technology

Volume 3 of 5

Strain Determination by Fiber Optics

Prepared by Missouri S&T
and Missouri Department of
Transportation



FINAL REPORT
RI02-022

**Preservation of Missouri Transportation Infrastructures:
Validation of FRP Composite Technology**
Volume 3
Strain Determination by Fiber Optics

Prepared for the
Missouri Department of Transportation
Organizational Results

In Cooperation with the
National University Transportation Center

by
Center for Infrastructure Engineering Studies
Missouri University of Science and Technology
Steve E. Watkins

September 2008

The opinions, findings and conclusions expressed in this report are those of the principal investigator and the Missouri Department of Transportation. They are not necessarily those of the U.S. Department of Transportation or the Federal Highway Administration. This report does not constitute a standard, specification or regulation.

TECHNICAL REPORT DOCUMENTATION PAGE

1. Report No. OR 09 - 009	2. Government Accession No.	3. Recipient's Catalog No.	
4. Title and Subtitle Preservation of Missouri Transportation Infrastructures: Strain Determination by Fiber Optics (Task V3. Load Tests and Monitoring Sub-Task 3.6)		5. Report Date September 2008	
		6. Performing Organization Code Missouri S&T	
7. Author/s Steve E. Watkins		8. Performing Organization Report No.	
9. Performing Organization Name and Address Center for Infrastructure Engineering Studies Missouri University of Science & Technology 223 Engineering Research Lab Rolla, MO 65409		10. Work Unit No. (TRAIS)	
		11. Contract or Grant No. DTRT06-G-0014	
12. Sponsoring Organization Name and Address U.S. Department of Transportation Research and Special Programs Administration 400 7 th Street, SW Washington, DC 20590-0001		13. Type of report and period covered Final	
		14. Sponsoring Agency Code MoDOT	
15. Supplementary Notes			
16. Abstract <p style="text-align: center;">Structural assessment of bridge P-0962 in MODOT District 8 involved both the sensing network of fiber-optic and electrical resistance strain gauges (ESGs). Sensing arrays were installed on the mid-span of the bridge to determine the performance of the fiber-optic strain sensors for field applications and to provide in situ measurement capability for the strengthened bridge. Extrinsic Fabry-Perot Interferometric (EFPI) strain sensors were used to measure point strain. Dynamic and static load tests were performed as well as finite element analysis. Scenarios are given for the load testing along with data filtering and processing details.</p>			
17. Key Words Bridge monitoring, FRP, in-situ load test, static load test, fiber-optic strain sensors, smart structural assessment, health monitoring.		18. Distribution Statement No restrictions. This document is available to the public through the National Technical Information Service, Springfield, Virginia 22161	
19. Security Classification (of this report) Unclassified	20. Security Classification (of this page) Unclassified	21. No. of Pages 37	22. Price Free

Form DOT F 1700.7 (8-72)

Reproduction of form and completed page is authorized

Table of Contents

1. INTRODUCTION	Pg. 7
2. BACKGROUND	Pg. 7
2.1. Fiber Optic Health Monitoring	Pg. 7
2.2. Strain Monitoring System	Pg. 9
3. EMBEDDED FIBER OPTIC INSTRUMENTATION	Pg. 10
3.1. Strain Monitoring Network	Pg. 10
3.2. Strain Monitoring Assessment Program	Pg. 11
4. LOAD-INDUCED STATIC AND DYNAMIC STRAIN RESULTS	Pg. 13
4.1. Dynamic Strain Results	Pg. 13
4.2. Static Strain Results	Pg. 18
5. AUTONOMOUS TESTING PLAN	Pg. 23
5.1. Smart Monitoring Protocol	Pg. 23
5.2. Timing Feasibility	Pg. 26
6. CONCLUSIONS	Pg. 28
6.1. Smart Strain Monitoring System	Pg. 28
6.2. Research Publication	Pg. 29
7. REFERENCES	Pg. 30

List of Illustrations

- Figure 1.** Sensor System: (a) Extrinsic Fabry-Perot Interferometric (EFPI) sensor with an external air-gap cavity and coated high-reflectance fiber surfaces. (b) EFPI fiber optic sensor and support instrumentation for absolute strain measurement. Pg.7
- Figure 2.** End schematic view of the sensor network. Pg. 9
- Figure 3.** Initial Rolling Load Test Results at location LR using Full Size Pickup. Pg. 13
- Figure 4.** Example Rolling Load Results at location TR from Full Scale Vehicle. Pg. 14
- Figure 5.** Unfiltered ESG with EFPI Rolling Load Signal. Pg. 14
- Figure 6.** Filtered ESG with EFPI Rolling Load Signal. Pg. 15
- Figure 7.** – Triggering System. (a) Truck and Bridge Configuration. (b) Detail of the Triggering Instrumentation. Pg. 23

List of Tables

- Table 1.** Dynamic Load Test Results. Pg. 12
- Table 2.** Dynamic Health Coefficients. Pg. 16
- Table 3.** Static Load Test Results. Pg. 17
- Table 4.** Static Health Coefficients. Pg. 18
- Table 5.** Static Strain (Finite Element Analysis). Pg. 19
- Table 6.** Comparison of FEA and Measured EFPI Results. Pg. 20
- Table 7.** Photoeye Detection Range with Hood. Pg. 24
- Table 8.** Timing Statistics. Pg. 25

1. INTRODUCTION

Fiber optic strain sensors offer benefits for permanent health monitoring applications. This work involved the implementation of a network of fiber optic strain sensors on bridge P-0962. The sensing network monitored strain at the midspan in the center bay of the bridge. The sensor array was primarily intended to confirm the structural strengthening and to monitor performance over time. The Extrinsic Fabry-Perot Interferometric (EFPI) strain sensor was the target sensor type. Research issues included comparison of the EFPI sensors to traditional electrical gages, comparison of the EFPI sensors to the analytical results, and accommodation for the field application (e.g. temperature, aging, and failure). Practical problems of installation and feasibility of intelligent monitoring are also explored.

2. BACKGROUND

2.1. Fiber Optic Health Monitoring

Health monitoring technology for civil engineering infrastructure has developed during the last decade [1-12]. Smart structures instrumentation consists of permanent, integral sensors to measure key parameters such as strain and deflection [1-3, 13]. Benefits include enhanced understanding of in-service conditions, verification of repair or upgrades, and improved management of service life. A current area of research is field validation of sensing techniques using in-service structures and the development of associated dedicated instrumentation. Fiber optic strain sensors can provide field measurements related to load performance and structural health [14] and have advantages

of environmental ruggedness, low profile, and high sensitivity [3, 13, 15-17]. Such fiber optic sensors offer excellent sensitivity, durability, embeddability, and are virtually immune to electromagnetic interference [13, 18]. Embedded fiber-optic sensor networks are good candidates for long-term installations where durability, extended life expectancy, and long term accuracy are required. The Fabry-Perot cavity gives a highly responsive, and noise-free, sensing device that performs well in field conditions [6, 10-12, 18-22]. Fiber optic sensors have been used in fiber-reinforced-polymer (FRP) composite, reinforced-concrete (RC), and steel structures [5, 6, 10-12, 18, 23, 24] to monitor internal strains for selected locations.

Using the component technologies developed for the telecommunications industry, fiber optic systems have been proposed, developed, and commercialized for many sensing applications. These sensors offer wide range of advantages over non-optical sensors including little perturbation to the host structure, good fatigue performance, and the ability to form multiplexed networks for complex measurements. Advances in fiber optic sensing technology are reducing the weight, required power, and the cost. Fiber optic sensors are ideal for smart civil structures applications because they may be embedded in the FRP materials to measure internal conditions and they can provide absolute measurements without the need for continuous monitoring. Their fatigue performance is desirable for applications requiring permanent structural sensors. The sensors have an extended lifetime in extreme environments when incorporated properly in a structure. In particular, they are resistant to vibration and temperature.

2.2. Strain Monitoring System

The Extrinsic Fabry-Perot Interferometric (EFPI) sensor is a type of fiber optic sensor that is capable of reliable strain measurement [25-30]. An EFPI fiber optic sensor is schematically shown in Figure 1(a). Figure 1(b) displays the schematic of source/detector system for the EFPI fiber optic sensors.

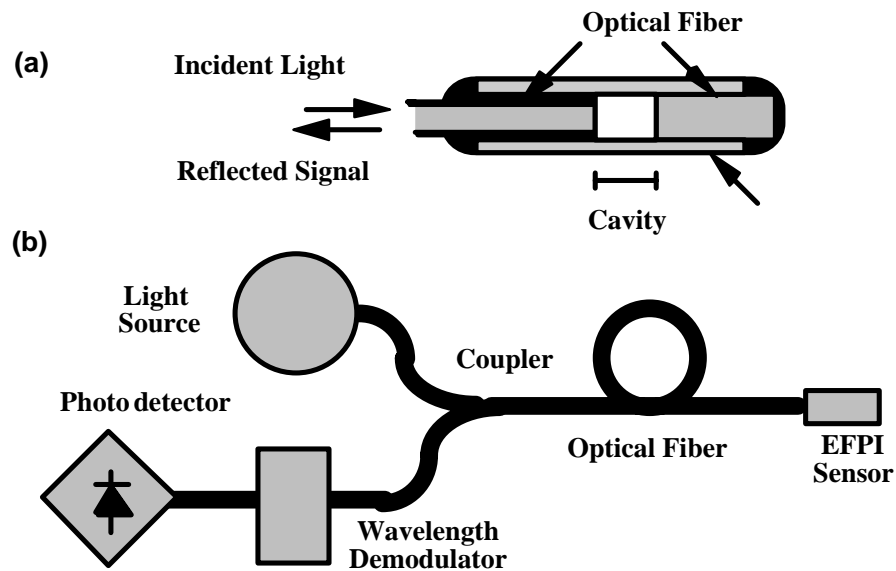


Figure 1. Sensor System: (a) Extrinsic Fabry-Perot Interferometric (EFPI) sensor with an external air-gap cavity and coated high-reflectance fiber surfaces. (b) EFPI fiber optic sensor and support instrumentation for absolute strain measurement.

The EFPI fiber optic sensor utilizes multiple-beam interference between two polished end-faces of a single mode fiber and a multimode fiber. A capillary tube is bonded to the two fibers and maintains the alignment of their end faces. The tube is bonded to a material under strain. As the material and attached tube are strained, the reflected interference signal varies in response to changes in cavity spacing. The gage length is

determined by the length of this capillary tube rather than the cavity and can be built to varying lengths around one centimeter to one-half centimeter. It can measure absolute strain over a small gage length with little transverse coupling, i.e. the measurement effectively gives the axial component of strain [24]. It can be surface mounted or embedded. In the support instrumentation, a light-emitting-diode source provides the input light beam into the single mode fiber. A coupler and wavelength demodulator branches the reflected interference fringes to a detector. The interference response at several wavelengths can determine the absolute cavity displacement and hence the absolute strain. The instrumentation (model AFSS) was manufactured by Luna Innovations. Standard high-finesse sensors will be used. The fatigue, noise, and sensitivity characteristics are excellent [24, 29-30].

3. EMBEDDED FIBER OPTIC INSTRUMENTATION

3.1. Strain Monitoring Network

An EFPI sensor array and a co-located array of ESGs were installed on bridge P-0962 in summer of 2003. In Figure 2, the sensing network locations are shown. The sensing network monitored strain at the midspan in the center bay of the bridge. The bridge runs North-South and the network was installed in the western side of the bridge. Two sensor locations were on the longitudinal beam. Two EFPI sensors and an ESG measured longitudinal strain within the layers of the FRP wrap (location designated LW). Co-located sensors measured longitudinal strain in the internal steel rebar at the bottom of the beam (location designated LR). Two additional sensor locations were on the underside of the road deck midway between the longitudinal beams. Co-located sensors measured

transverse strain within layers of the FRP wrap (location designated TW). Sensors measured transverse strain in the internal rebar at the bottom of the deck (location designated TR). In each sensor location the two EFPI sensors and the ESG were co-located within three linear inches of each other. Sensor installation was attempted on the concrete underneath the paved wear surface of the bridge; these sensors behaved unreliably (e.g. tensile and compressive strain for similar loadings and complete ESG unresponsiveness by the second load test) and are omitted from the tests results. All sensor cables are embedded and terminated in a control box mounted to the bridge. Instrumentation for the EFPI sensors and the ESG were patched through the control box during the load tests.

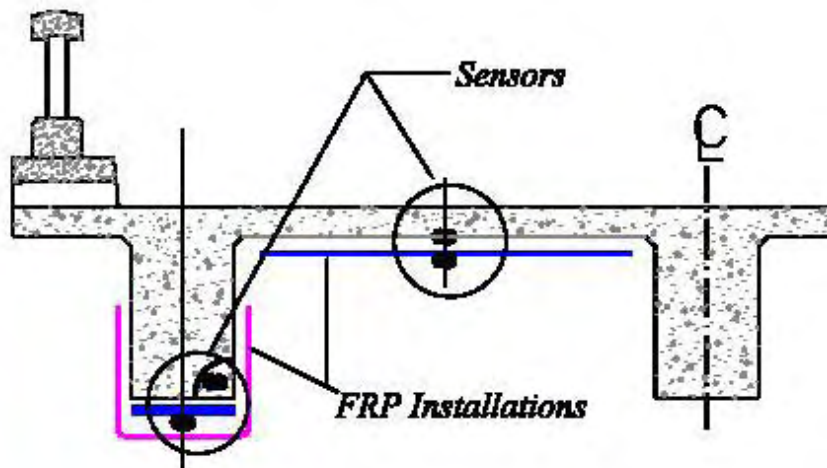


Figure 2. End schematic view of the sensor network.

3.2. Strain Monitoring Assessment Program

Structural assessment of bridge P-0962 in MODOT District 8 involved both the sensing network of fiber-optic and ESGs. These systems have good directional properties and are

effectively point sensors. Scenarios are given in the next section for the load testing along with data filtering and processing details.

EFPI sensors and ESGs have similar applications, but they differ in important respects. The fiber optic sensor can be embedded within concrete or FRP materials with more ease and longevity than the ESGs. The EFPI sensors have a smaller profile and can be embedded into tighter places. EFPI systems provide much more accuracy and potential measurement bandwidth than the ESG systems as well. The accuracy and bandwidth of ESG sensors is dependent on the construction of the amplifier and filtering circuitry. EFPI systems also are dependent on electronic circuitry; however the actual sensor resolution and bandwidth are dependent on fiber-optic parameters. Resolution therefore is dependent on the wavelength of the fiber-optic systems. The EFPI bandwidth is dependent on the processing speed of the instrumentation. The normal processing that is required for these systems is based digital-signal-processing (DSP) technology and therefore the bandwidth will be dependent on the speed and bit-resolution of the DSP subsystem.

A commercial fiber-optic sensor system from Luna Innovations (model Fiber Pro) was used to demodulate the sensor readings for the EFPI sensors. The Fiber Pro was capable of 1000 Hz sampling and sub-microstrain resolution. Through a computer interface, the information was captured to a text file for further processed with Excel or Matlab. In this work, Model AFSS high-finesse EFPI sensors from Luna Innovations were used with a wavelength of 830 nm and a gauge length of approximately 8 mm.

In ESG systems, the strain was detected by deformation in a resistive grid element. This technology is mature and an ESG is typically interrogated with a wheatstone bridge

and amplifier circuitry. For this project, a dedicated Missouri S&T multi-channel system was used. The PC-based National Instruments data acquisition operated at a 1000 Hz sampling rate on each channel. Post-test signal processing was done on the recorded strain, e.g. filtering. The ESGs used in the bridge are Model EA-06-250BG-120 electrical resistance gauges from Micro-Measurements Company. These gauges had a nominal resistance of 120 Ω and a gauge length of 6.35 mm and 50.80 mm, respectively.

4. LOAD-INDUCED STATIC AND DYNAMIC STRAIN RESULTS

Two loading scenarios were used for this study; a dynamic rolling load and a static load. After sensor network installation and bridge strengthening in 2003, the load tests were conducted on 11/10/2004 and 10/20/2005. Dynamic rolling loads were performed with a full-size pickup as well as a full-scale H-20 load test vehicle. These dynamic tests were used to check the operability and sensitivity of the sensor network as well as providing a baseline of the dynamic behavior of the bridge. Static loadings were performed using a full-scale loading vehicle with the heavy axle over mid-span as described in the standard published by the American Association of State Highway and Transportation Officials (AASHTO). This type of load was used to evaluate the strength of the structure with respect to time, i.e. assess the strengthening and aging.

4.1. Dynamic Strain Results

Initial rolling load tests were performed with a full-size pickup. These tests showed that the EFPI sensor network was performing at 11.25 percent of the bridge load rating (16,014 N, 3600 lbs). The EFPI sensors were showing clear patterns for strains less than 10 microstrain .

Dynamic loading consisted of passing a weighted H-20 vehicle over each lane of traffic in the proper direction and then over the center lane in both directions. The lanes of travel on the structure were WL-SB for the west lane south bound, EL-NB for east lane north bound, and CL for the center lane of travel. The sensor network captured the strain profile that was generated by the rolling loads in each lane of travel.

Rolling load tests were performed by passing the test vehicle over the structure at a slow speed to ensure that sufficient strain detail is sampled. This test allowed for assessment of structural behavior as a vehicle passes. For realistic velocities, the sampling rate on the EFPI system would need to be greater than that available at the time of this work. The peak loads for these dynamic tests are summarized in Table 1.

Table 1. Dynamic Load Test Results.

	WL-SB Peak		CL-SB Peak		EL-NB Peak	
	November 10 th , 2004					
	FR (Rebar) [$\mu\epsilon$]	TW (FRP) [$\mu\epsilon$]	LR (Rebar) [$\mu\epsilon$]	TW (FRP) [$\mu\epsilon$]	LR (Rebar) [$\mu\epsilon$]	TW (FRP) [$\mu\epsilon$]
ESG	X	X	57.85	49.24	38.30	54.88
FOSS	81.17	51.92	35.15	62.18	30.03	42.56
October 20 th , 2005						
ESG	X	X	109.03	31.22	93.17	18.14
FOSS	58.93	63.03	61.20	54.96	95.66	107.65

The initial rolling load test of rebar strain taken at a low sampling rate is shown in Figure 3. This data shows that the sensor array is active and sensitive to light loads, e.g. 11.25 percent AASHTO load. The EFPI instrumentation had a minimum resolution of 1 microstrain and the ESG system data was filtered as discussed in the next subsection. Figure 4 shows a load signature for the rebar strain from a transversely mounted sensor. Both the front and rear axle contributions to the signature were apparent for the full-scale H-20 vehicle. Note the two strain peaks were due to the front and rear axles of the truck.

Filtering of data is often employed to remove unwanted noise. In this case, the ESG sampled data was filtered to remove noise from over-sampling or outside interference. A second-order discrete-time butterworth filter was determined and used to filter the data during post-processing. The transfer function of the filter is shown in the equation. Examples of strains before and after filtering are shown in Figures 5 and 6 for the sensors at location LR. Note that the longitudinal beam did not show the double peak pattern. Figure 5 compares ESG results in which no post-processing is performed on the data and the EFPI sensor results. Figure 6 shows the filtered results alongside the EFPI system results. Note that no filtering is required for the EFPI data.

$$H(s) = \frac{s^2 - 1.956s + 0.9565}{0.0002414s^2 + 0.0004827s + 0.0002414}$$

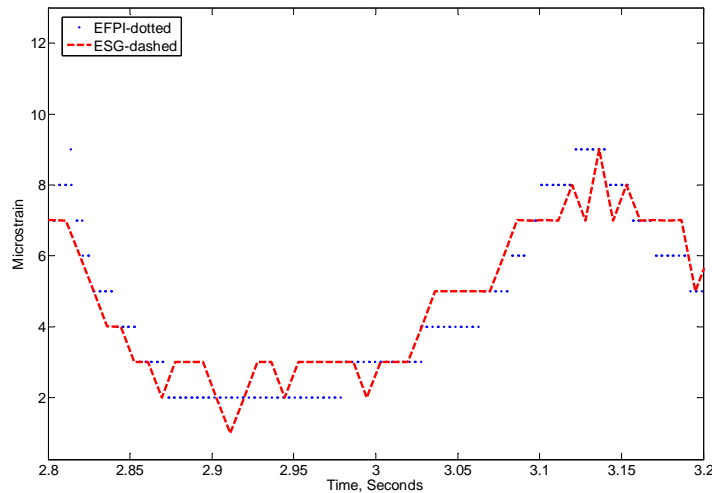


Figure 3. Initial Rolling Load Test Results at location LR using Full Size Pickup.

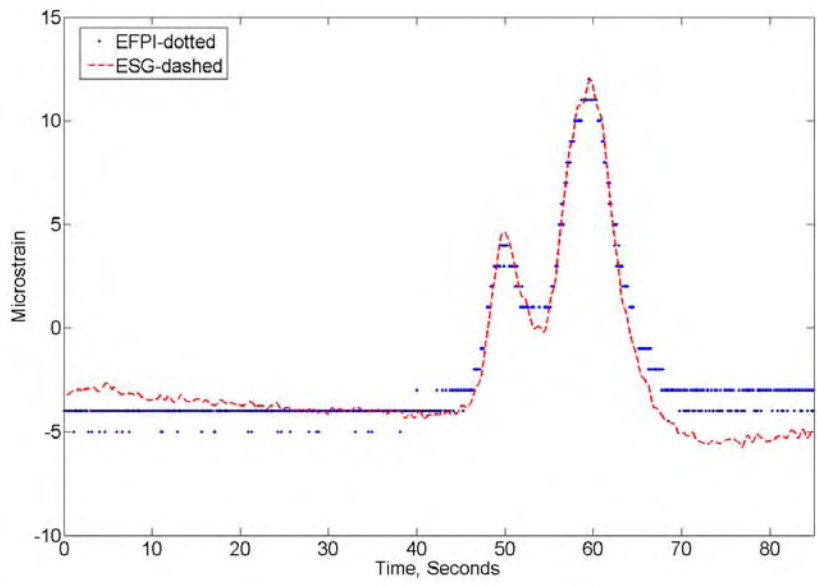


Figure 4. Example Rolling Load Results at location TR from Full Scale Vehicle.

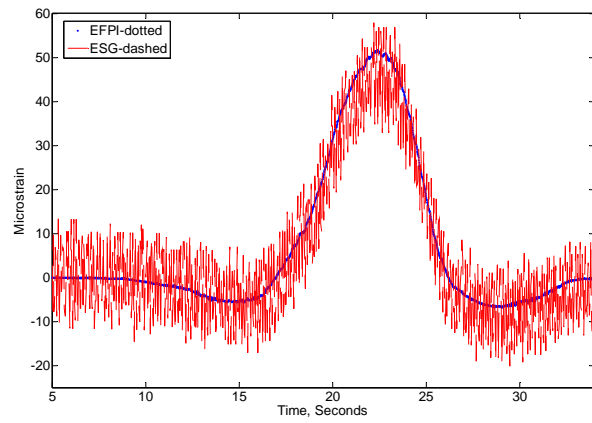


Figure 5. Unfiltered ESG with EFPI Rolling Load Signal.

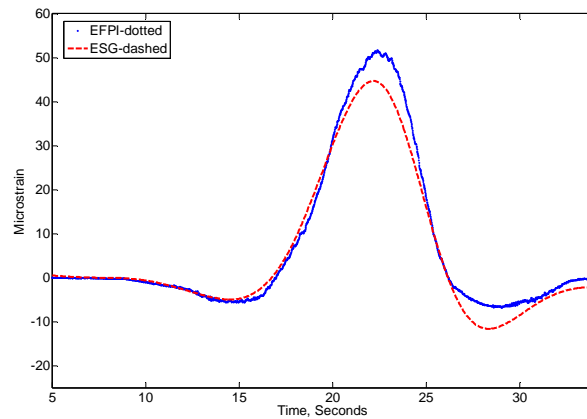


Figure 6. Filtered ESG with EFPI Rolling Load Signal.

The EFPI sensors and system demonstrated better operating characteristics than the co-located ESGs. Once operating after installation, the EFPI sensors did not fail during this two-year test and these sensors show consistent performance with age, while the ESG network showed sensor failures. EFPI systems can provide increased accuracy as their least-count measurement is determined by the operating wavelength. Electromagnetic noise on an EFPI systems is also unlikely to be introduced in the cabling since fiber optics are immune to such interference. ESGs are inherently noisier due in part to antenna loops in the runs of copper cabling and they require more post-processing than their EFPI counterparts, especially in a field application.

Health coefficients were proposed to track the condition of the structure over time. Health coefficients were calculated to compare the performance among load tests. Using the load ticket information, the strain information was normalized. The equation shows the calculation of health coefficients Γ . For both dynamic and static values, ϵ_{peak} was the peak strain observed and W was the rear-axle weight in kilo-Newtons. The peak strain values for dynamic cases were taken from the maximum peak in double-peak patterns.

The ESG peak strain values for both cases were taken after the data was filtered. Table 2 shows the health coefficients for the dynamic loading case.

$$\Gamma = \frac{|\mathcal{E}_{peak}|}{W}$$

This health coefficient equation was not ideal, however it may be sufficient to track structural degradation. It normalized the strains to the rear-axle weight. The weights of the rear axles were directly over the sensor locations for peak strain. However, the strain values were influenced by the entire weight. The exact normalizing “weight” was presumably a complicated function of the type of test and the sensor location. For instance, the dynamic sensor values in the longitudinal beam showed only one peak (per the entire weight) and the values for the transverse deck showed two semi-independent peaks from the front and rear axles. The development of a more accurate health coefficient equation was beyond the scope of this work.

Table 2. Dynamic Health Coefficients.

	WL-SB Peak		CL-SB Peak		EL-NB Peak	
	November 10 th , 2004					
	LR (Rebar) [μɛ/kN]	TW (FRP) [μɛ/kN]	LR (Rebar) [μɛ/kN]	TW (FRP) [μɛ/kN]	LR (Rebar) [μɛ/kN]	TW (FRP) [μɛ/kN]
ESG	X	X	0.294	0.250	0.195	0.279
FOSS	0.413	0.264	0.179	0.316	0.153	0.216
October 20 th , 2005						
ESG	X	X	0.499	0.143	0.426	0.083
FOSS	0.270	0.288	0.280	0.252	0.438	0.493

4.2. Static Strain Results

Static load results for averaged and filtered strains over approximately 30-second intervals are shown in Table 3. The H-20 AASHTO truck was positioned with the heavy axle over the mid-span in the center bay. The ESG at location TR completely failed

between the first and second load tests and the ESGs at locations LR and TW produced questionable values for all measurements in the second load test. The EFPI sensors that were operating after installation gave reasonable results in all tests.

Table 3. Static Load Test Results.

	Longitudinal Beam		Transverse Deck	
	November 10 th , 2004			
	LW (FRP) [$\mu\epsilon$]	LR (Rebar) [$\mu\epsilon$]	TW (FRP) [$\mu\epsilon$]	TR (Rebar) [$\mu\epsilon$]
ESG	53.35	75.90	112.40	56.32
FOSS	48.43	42.61	21.68	59.69
	October 20 th , 2005			
ESG	69.88	105.57	-9.90	X
FOSS	51.39	-23.04	26.86	25.97

The load tests gave insight into the behavior of the bridge and performance of the sensor network. The bridge had been strengthened by the FRP wrap and had a higher load rating. Comparison of EFPI strain measurements between the 2004 and 2005 tests showed that the strains in the longitudinal beam were more consistent than the strains in the transverse deck and that the static strains were more consistent than the dynamic strains. The deck was presumably more sensitive to load position than the longitudinal beam and the load placement was much less certain for the dynamic tests than for the static tests. Also, the rebar locations showed some variation even for the EFPI sensors, but this behavior was not unexpected due to load redistribution as the concrete cracks with time. Structural health can be quantified using the strain monitoring. For instance, a significant change in static strains would indicate structural degradation.

The EFPI sensors showed consistent performance during the two years of testing. All EFPI measurements were reasonable. No EFPI fiber-optic sensor that was installed successfully failed during the course of the study. However, the ESG sensor network had

started to fail and the performance degradation was not associated with only sensors experiencing high strain levels. Only the ESG at LW gave reliable results during the second test and the ESG at TR was completely unresponsive. The LR and TW ESGs produced erratic and inconsistent measurements. The failure cause was not clearly understood, but it seems to be associated with aging.

Health coefficients were calculated to compare the performance among static load tests. The calculation of health coefficients Γ was done just as the calculations for the dynamic tests. The ESG peak strain values for both cases were taken after the data was filtered. Table 4 shows the health coefficients for the static loading case. The performance was similar to the dynamic case.

Table 4. Static Health Coefficients.

	Longitudinal Beam		Transverse Deck	
	November 10 th , 2004			
	LW (FRP) [$\mu\epsilon$]	LR (Rebar) [$\mu\epsilon$]	TW (FRP) [$\mu\epsilon$]	TR (Rebar) [$\mu\epsilon$]
ESG	0.271	0.386	0.572	0.286
FOSS	0.246	0.217	0.110	0.304
	October 20 th , 2005			
ESG	0.320	0.483	0.045	X
FOSS	0.235	0.105	0.123	0.119

A Finite Element Analysis (FEA) was performed to model the expected performance of the strengthened bridge for a static load test. The model consisted of three-dimensional solid elements that represented the deck, girders, and parapets acting as a composite structure. The FEA was implemented by using the commercial software Abaqus version 6.4. A linear elastic analysis was performed for the load configuration of the static load test performed on the middle bay of the bridge. The Finite Element used for the simulations was the so-called “C3D8” which is a continuum (solid) three-dimensional

element that has eight nodes with three active degrees of freedom (DOF) per node. The active DOFs of this element are the translations along each of the global coordinate axes (x-, y-, and z-axis). The concrete of the deck, girders, and parapets was modeled as having a compressive strength f'_c equal to 6850 psi. The modulus of elasticity of the concrete was defined as $E_C = 57,000(f'_c)^{1/2}$. The Poisson's Ratio (ν) was assumed to be 0.20. The FEA loads were modeled as concentrated loads per the experimental truck locations.

Table 5 shows the FEA results corresponding to the static tests from the 11/10/2004 and 10/20/2005 load tests. The strains in the top of the bridge at each designated location in the longitudinal beam and the transverse deck are also given. FEA results show that the structure was a stiffer structure than before strengthening. Note that the predicted top strains were negative and small; the unreliable results of the top sensors may be due to faulty sensor bonding or to some complex interaction in the road surface. This question should be explored in future research. The FEA results are directly compared to the EFPI results in Table 6. The percent difference was calculated as

$$\% Diff = \left(\frac{\varepsilon_{EFPI} - \varepsilon_{FEA}}{\varepsilon_{FEA}} \right) \cdot 100$$

Table 5. Static Strain (Finite Element Analysis).

Date	Longitudinal Beam			Transverse Deck		
	LW (FRP) [$\mu\varepsilon$]	LR (Rebar) [$\mu\varepsilon$]	Top [$\mu\varepsilon$]	TW (FRP) [$\mu\varepsilon$]	TR (Rebar) [$\mu\varepsilon$]	Top [$\mu\varepsilon$]
11/10/2004	89.0	73.0	-24.0	39.0	27.0	-20.0
10/20/2005	96.0	84.0	-34.0	42.0	29.3	-27.0

Table 6. Comparison of FEA and Measured EFPI Results.

	Longitudinal Beam		Transverse Deck	
	November 10 th , 2004			
	LW (FRP) [$\mu\epsilon$]	LR (Rebar) [$\mu\epsilon$]	TW (FRP) [$\mu\epsilon$]	TR (Rebar) [$\mu\epsilon$]
ESG	89.0	73.0	39.0	27.0
EFPI	48.43	42.61	21.68	59.69
% Difference	45.58	41.63	44.41	121.07
	October 20 th , 2005			
ESG	96.0	84.0	42.0	29.3
EFPI	51.39	23.04	26.86	25.97
% Difference	46.47	72.57	36.05	11.37

The load-induced strain measurements from the EFPI sensors showed general agreement with the comparison sensors and showed similar trends with the FEA results. The measurements were very close considering differences in load placement and the non-zero distances between co-located sensors. In particular, the proposed EFPI static health coefficients were consistent for similar locations for the two tests. Also, the FEA results were uniformly higher than EFPI measurements with one rebar exception. FEA analysis verified that the structure was strengthened after rehabilitation since EFPI and ESG readings showed strains corresponding to a stiffer structure. Hence, the bridge showed greater stiffness than the analytical predictions and the EFPI sensors tend to measure strain at a similar fraction of the corresponding analytical predictions. Consequently, all EFPI results appeared to be reasonable and to have the potential for effectively quantifying bridge performance.

As permanent instrumentation, the EFPI fiber-optic system displayed uniform performance during annual dynamic and static load tests. This sensor type and system displayed excellent longevity, sensitivity, and accuracy. This work provided field validation of these characteristics. The EFPI sensors and system demonstrated better

operating characteristics than the co-located ESGs. Once operating after installation, the EFPI sensors did not fail during this two-year test and these sensors showed consistent performance with age, while the ESG network showed sensor failures. Electromagnetic noise on EFPI systems was also unlikely to be introduced in the cabling. ESGs were inherently noisier due in part to antenna loops in the runs of copper cabling and they required more post-processing than their EFPI counterparts, especially in this field application. The following observations were noted during the work.

- The bridge behavior per the fiber-optic measurements seemed to show more repeatable results in the longitudinal beam than the transverse deck locations. The cause may be more sensitivity to load placement and the environment.
- A proposed health coefficient showed promise as a single measure of load performance, but needs more development related to loading details and correlation with bridge condition and aging as future tests are performed.

5. AUTONOMOUS TESTING PLAN

5.1. Smart Monitoring Protocol

Improvements in quantitative bridge monitoring for management and assessment of damage must address economy and speed issues as well as provide assurance of safety and performance. Quantitative systems must accommodate periodic measurements over the life of the bridge with limited expense and power requirements, at least for the embedded hardware. They must accomplish their measurements with reduced cost and time. They must allow for rapid assessment of performance e.g. to limit traffic disruption and road closure. Intelligent processing must be integrated to provide interpretation to

the measured data for the non-specialist users.

A smart structures approach to field monitoring system for bridges has three components. 1) The sensor, or sensors, should be capable of providing a well-understood measure of bridge integrity. The fiber optic strain sensor array has been shown to provide reliable, long-term strain measurements. 2) The data acquisition should be accompanied by sufficient processing to address interpretation and data acquisition requirements. For embeddable sensor motes or wireless sensor nodes, the processing may include calibration, noise elimination, etc. and the data acquisition can be done through wireless links. 3) The measurement component should automate as much of the test as possible. Setup time at the bridge and time for bridge closure should be minimized.

This development looked at the feasibility of an automated monitoring system for static load tests. The proposed smart system consisted of in-situ strain sensors, an embedded wireless sensor node, and a measurement triggering system. The sensors, the node, and a passive marker are mounted on the bridge. A companion control unit is mounted on the bridge load, i.e. a weighted truck, and consists of data acquisition hardware, a wireless transmitter/receiver, and the triggering instrumentation. The system assumed that a single mid-span measurement is needed, although the system could be easily modified for multiple simultaneous or sequential measurements. The proposed test could be conducted by a single operator, i.e. the driver of the load truck. For a busy bridge, a team may be needed to flag traffic during the test.

The test must be initiated by the driver. The proposed initial sequence of events follows:

- The driver wakes the system before the truck reaches the bridge,
- The driver enters the parameters including the test type and selected sensors,
- The driver requests a baseline measurement of strain,
- The driver slowly drives across the structure stopping when the triggering system indicates the proper position of the vehicle, and
- The instrumentation takes the desired measurement(s) through the wireless node(s).

The triggering system is autonomous in that the triggering instrumentation determines the correct load position and the control unit collects and evaluates the measurement data. A similar sequence can be done for a dynamic test. The setup and testing can be conducted in short time with minimal traffic disruption and road closure.

A key component of the autonomous trigger approach is the triggering sub-system. Consider an infrared transmitter/receiver that is included with the truck control unit and a passive infrared reflector that is mounted on the bridge railing. For the sub-system shown in Figure 7, the performance depends on the detection range and the separation distance.

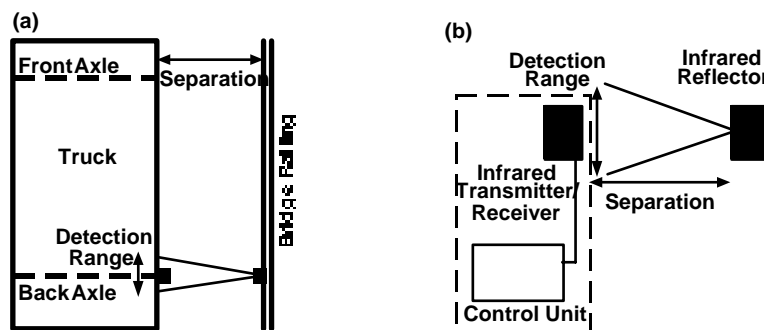


Figure 7. – Triggering System. (a) Truck and Bridge Configuration. (b) Detail of the Triggering Instrumentation.

The timing performance of the sub-system implementation was tested in the laboratory

using an infrared EMX NIRplus Retro-reflective Photoeye transmitter/receiver and a passive rectangular amber reflector of width 2.38 cm (15/16th inch) which is mounted in a non-reflective hood of depth 8.89 cm (3.5 inch) to meet directionality requirements. With this configuration, the detection range with the reflector hood is shown in Table 7.

Table 7. Photoeye Detection Range with Hood.

Photoeye/Reflector Separation	Detection Range
121.92 cm (48 inches)	5.715 cm (2.25 inches)
152.40 cm (60 inches)	7.3025 cm (2.875 inches)
82.88 cm (72 inches)	7.62 cm (3.0 inches)
213.36 cm (84 inches)	8.89 cm (3.5 inches)

5.2. Timing Feasibility

The response of the triggering sub-system must be sufficient to meet the requirements of the static testing protocols. The speed at which the Photoeye relay responds is the primary issue for timing. For static tests, the system personnel must be able to stop within the detection range if the load maintains a correct position and the triggering indicator remains on. (Note that the response time for the sensor nodes must be considered also. For sensor nodes used at Missouri S&T, sample collection can occur every 0.008 seconds if the network has been initialized. For this delay, the overall system timing is mainly constrained by the triggering component.) The timing statistics for 5000 tests are shown in Table 8.

Table 8. Timing Statistics.

STATISTICS FOR ALL Dt VALUES (sec)
Minimum = 0.02000
Maximum = 0.04550
Mean = 0.03174
Standard Deviation = 0.007441

Consider the 8.89-cm detection range. For the mean delay time of 0.031737 seconds, the truck will travel the 8.89-cm detection range at 10.1 kilometers-per-hour (6.3 miles-per-hour). This speed is a reasonable upper limit. For a more complex network and multiple loading positions, the static test protocol can easily be modified and these same trigger considerations used for proper positioning. The sequential sampling and timing performance will need more consideration in a dynamic test protocol. These preliminary laboratory results encourage development of a field system for testing.

Economical and rapid monitoring of bridges can promote safety and management of infrastructure. Quantitative information on performance provides a better assessment of health than qualitative inspections. However, cost issues associated with instrumentation hardware and time issues related to setup time and traffic disruption are practical limits to such advances. These issues are addressed by this autonomous approach. Much of the instrumentation can be located on the truck versus the bridge. In particular, just a passive infrared reflector is needed on the bridge for the triggering system. Also, the instrumentation is scaleable in that a single measurement can be made from one embedded module, multiple simultaneous measurements can be made from a network of modules, or multiple measurements can be made for a prescribed loading sequence. Future investigations can implement the system on field structures and can measure parameters for the entire integrated system.

6. CONCLUSIONS

6.1. Smart Strain Monitoring System

An EFPI fiber optic sensor array and a co-located ESGs array were installed on P-0962 in summer of 2003. Use of the sensor array was primarily intended for confirmation of the structural strengthening and for monitoring of the performance over time. Research issues included protocols for sensor installation, comparison of the EFPI sensors to the ESGs, comparison of the EFPI sensors to the FEA results, accommodation for the field application (e.g. temperature, aging, and failure), and processing needed for intelligent monitoring.

The EFPI array met expectations on performance. The installation protocol emphasized security of the network, e.g. protection from the environment and vandalism. The sensors and the network cabling were embedded. The sensor connections were made at a single access box. The fiber optic sensors, if successfully installed, provided reasonable strain information during the multi-year study and did not show aging failure. The fiber optic sensor results correlated well with the results from the co-located electrical resistance gages and from the computed finite element analysis. Static load measures met expectations. Dynamic load measures showed promise for providing insight into bridge performance. A proposal for more autonomous testing procedures was developed based on the longevity of the embedded sensor network and the capabilities of sensor node technologies.

